

CP violation studies at CMS

Aleksandr Tulupov^{1,2}, Sergey
Polikarpov^{1,2}

1 – NRNU MEPhI

2 – LPI RAS

On behalf of the CMS Collaboration

ICPPA-2024 conference

Introduction

CPV in $D^0 \rightarrow K_S^0 K_S^0$

$B_S^0 \rightarrow J/\psi K_S^0$ effective lifetime

Conclusion

CPV – one of the Sakharov's necessary conditions for a Baryon asymmetry of the Universe generating

CP-violation is allowed in the SM, but the amount is insufficient to account for the observed BAU

Sources of CPV beyond the SM have to exist

CPV observables are often precisely predicted, hence, they are very sensitive to new physics

1. Direct CPV in decays $\Gamma(P \rightarrow f) \neq \Gamma(\bar{P} \rightarrow \bar{f})$
2. Indirect CPV in oscillations
3. Interference: CPV in decays + oscillations

We present the results of recent CMS measurements of

1. Direct CPV in charm
2. Lifetime measurement of the B_s^0 decay to CP-odd state (useful for better understanding of CPV in mixing)

CPV in $D^0 \rightarrow K_S^0 K_S^0$

[arXiv:2405.11606](https://arxiv.org/abs/2405.11606)

In contrast to strangeness and beauty, CPV is suppressed in charm

Theoretical SM calculations^[1] predict CPV in $D^0 \rightarrow K_S^0 K_S^0$ to be as large as $O(1\%)$ ← more significant than in many other D^0 decay channels

Latest experimental calculation by LHCb^[2]

$$A_{CP}(D^0 \rightarrow K_S^0 K_S^0) = (-3.1 \pm 1.2 \pm 0.4 \pm 0.2)\% \leftarrow \text{no CPV}$$

This work is the first CPV in charm sector at CMS

$$A_{CP} = \frac{\Gamma(D^0 \rightarrow f) - \Gamma(\overline{D}^0 \rightarrow f)}{\Gamma(D^0 \rightarrow f) + \Gamma(\overline{D}^0 \rightarrow f)}$$

$$A_{CP} \simeq A_{CP}^{raw} - A_{CP}^{production} - A_{CP}^{detector}$$

$$A_{CP}^{raw} = \frac{N(D^0 \rightarrow f) - N(\overline{D}^0 \rightarrow f)}{N(D^0 \rightarrow f) + N(\overline{D}^0 \rightarrow f)}$$

Many systematic uncertainties in A_{CP} cancel if measured via ΔA_{CP}

$$\Delta A_{CP} = A_{CP}^{raw}(D^0 \rightarrow K_S^0 K_S^0) - A_{CP}^{raw}(D^0 \rightarrow K_S^0 \pi^+ \pi^-)$$

Flavor tagging: $D^{*\pm} \rightarrow D^0(\overline{D}^0)\pi^\pm$

Signal events extraction

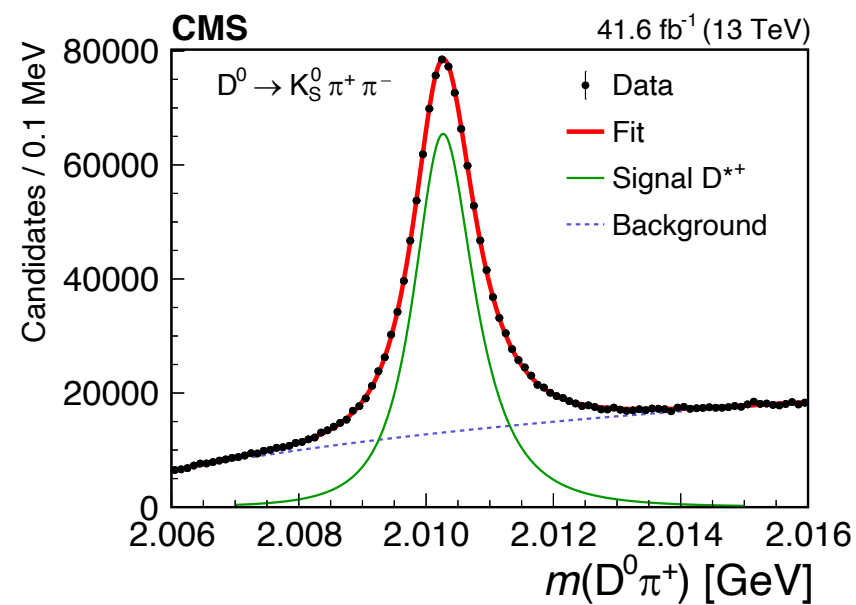
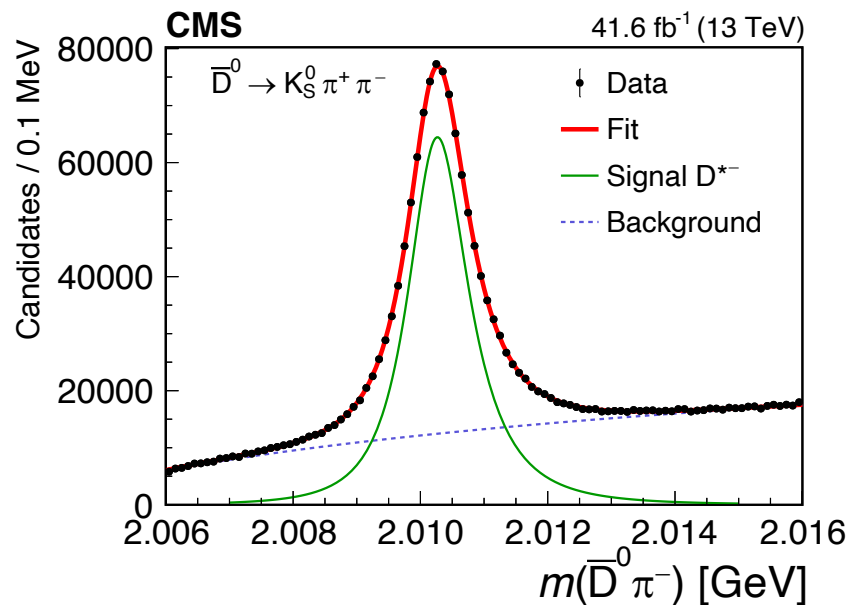
7

Signal events were selected using cut-based method

Fits of “+” and “-” are simultaneous: all parameters are shared, yields are floating

1D UML fit of $(M(D\pi^\pm) - M(D) + M_D^{PDG})$ is performed

Resulting $A_{CP}^{raw}(K_S^0\pi^+\pi^-) = (0.78 \pm 0.10)\%$

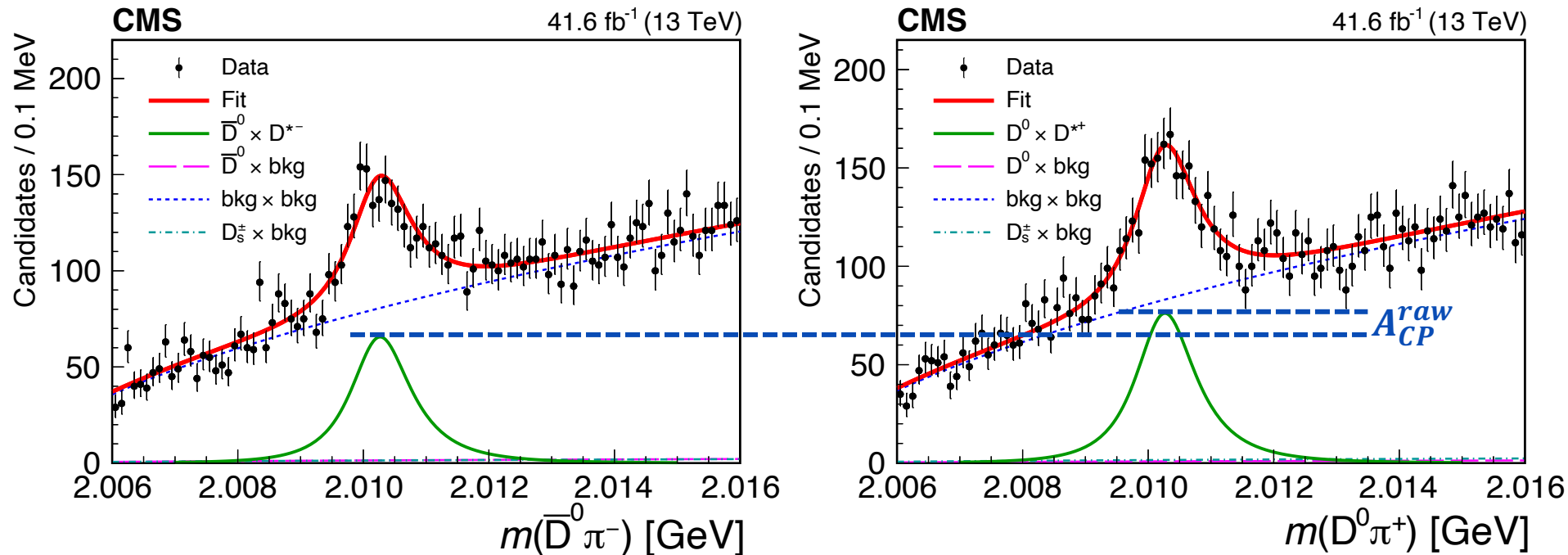


Signal events extraction

Fits of “+” and “-” are simultaneous: all parameters are shared, yields are floating

2D UML fit of $(M(D\pi^\pm) - M(D) + M_D^{PDG})$ and $M(K_S^0 K_S^0)$ performed

Resulting $A_{CP}^{raw}(K_S^0 K_S^0) = (7.1 \pm 3.0)\%$



$A_{CP}^{raw}(K_S^0 K_S^0)$ is measured

$$A_{CP}^{raw}(K_S^0 K_S^0) = (7.1 \pm 3.0)\%$$

ΔA_{CP}^{raw} is calculated using following expression

$$\Delta A_{CP}^{raw} = A_{CP}^{raw}(D^0 \rightarrow K_S^0 K_S^0) - A_{CP}^{raw}(D^0 \rightarrow K_S^0 \pi^+ \pi^-)$$

After all ΔA_{CP}^{raw} is measured

$$\Delta A_{CP}^{raw} = (6.3 \pm 3.0(stat) \pm 0.2(syst)) \%$$

Using PDG $A_{CP}^{PDG}(D^0 \rightarrow K_S^0 \pi^+ \pi^-)$, we derive:

$$A_{CP}(D^0 \rightarrow K_S^0 K_S^0) = \left(6.2 \pm 3.0(stat) \pm 0.2(syst) \pm 0.8(A_{CP}^{PDG})\right) \%$$

The first measurement of CP-violation in charm in CMS

$$A_{CP}(D^0 \rightarrow K_S^0 K_S^0) = \left(6.2 \pm 3.0(\text{stat}) \pm 0.2(\text{syst}) \pm 0.8(A_{CP}^{PDG}) \right) \%$$

The result is consistent with no CPV in $D^0 \rightarrow K_S^0 K_S^0$ at 2.0σ

The value is consistent with [LHCb^{\[2\]}](#) results at the level of 2.7σ
 $(6.2 \pm 3.1)\% \text{ vs. } (-3.1 \pm 1.3)\%$

and with [Belle^{\[3\]}](#) measurement at the level of 1.8σ
 $(6.2 \pm 3.1)\% \text{ vs. } (0.0 \pm 1.5)\%$

$B_S^0 \rightarrow J/\psi K_S^0$ effective lifetime

[arXiv:2407.13441](https://arxiv.org/abs/2407.13441)

This analysis presents a measurement of the B_s^0 effective lifetime τ in the CP-odd final state $J/\psi K_S^0$ with the CMS Run 2 dataset.

As soon as $J/\psi K_S^0$ is CP-odd state, neglecting CPV in B_s mixing $\tau(B_s^0 \rightarrow J/\psi K_S^0)$ is $\tau(B_{s,H})$

This allows us to accurately measure the B_s^0 heavy-state lifetime, which is useful for understanding the mixing in B_s^0 mesons

The proper decay time t of the B meson candidate is determined using

$$\tau = m \frac{\vec{L}_{xy} \cdot \vec{p}_T^B}{(\vec{p}_T^B)^2}$$

\vec{L}_{xy} is the vector in the transverse plane from the beamline to the B meson candidate fitted decay vertex

\vec{p}_T^B - transverse momentum of the B candidate

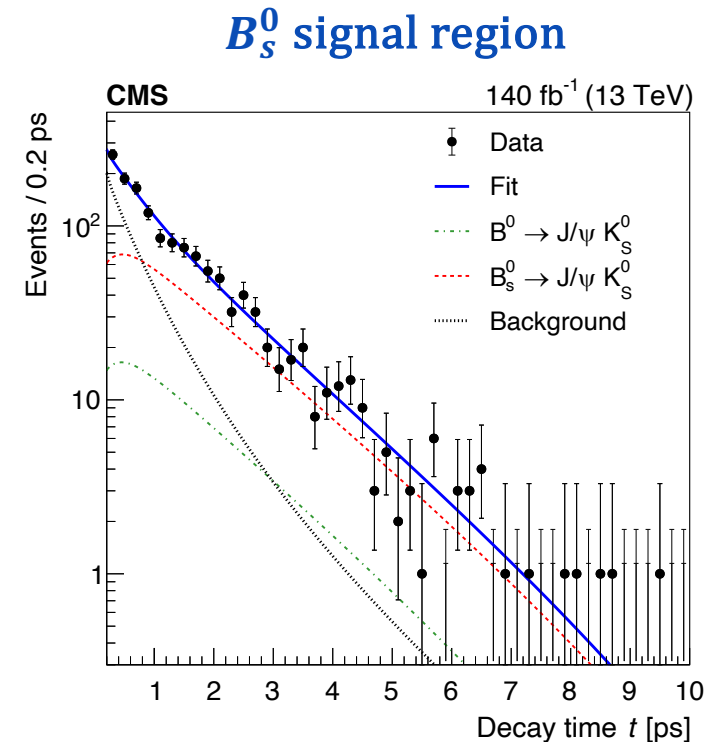
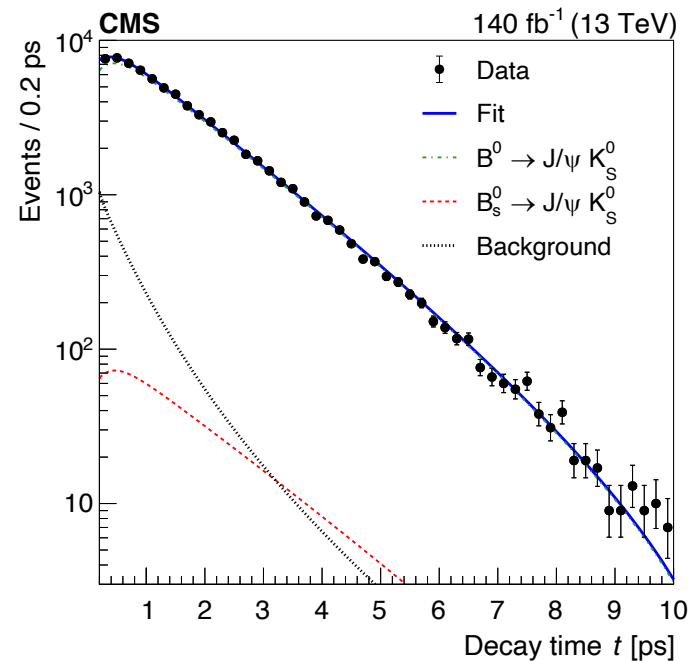
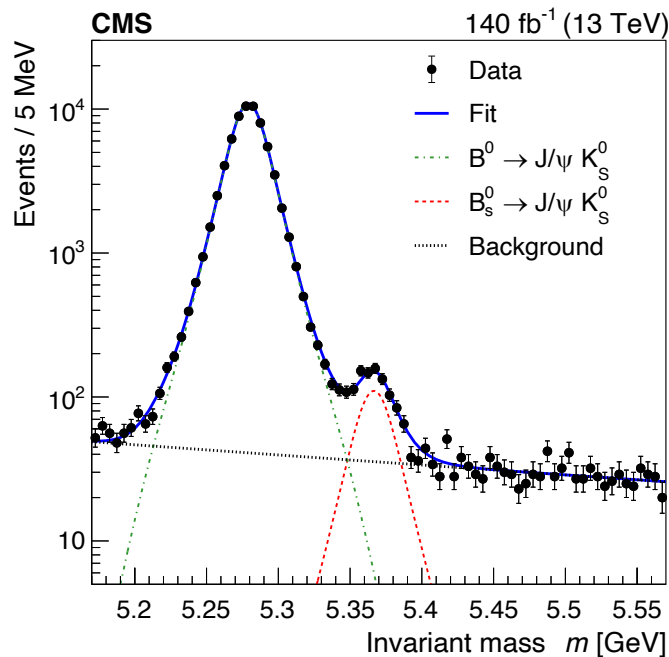
m - invariant mass of the B candidate

$B^0 \rightarrow J/\psi K_S^0$ - control channel for various bias tests and validations

Preprocessing: cut-based + BDT trained with 8 discriminating variables

2D UML fit to the $m(J/\psi K_S^0)$ and proper decay time

Both B_S^0 and B^0 are fitted



Using the latest measurements and assuming the SM:

$$\tau^{SM}(B_s^0 \rightarrow J/\psi K_S^0) = 1.62 \pm 0.02 \text{ ps}$$

Available **measurement from LHCb**^[4]:

$$\tau^{LHCb}(B_s^0 \rightarrow J/\psi K_S^0) = 1.75 \pm 0.14 \text{ ps}$$

The control channel 's effective lifetime is found to be in good agreement with the world-average value.

The measurement of B_s effective lifetime:

$$\tau(B_s^0 \rightarrow J/\psi K_S^0) = 1.59 \pm 0.07 \text{ (stat)} \pm 0.03 \text{ (syst)} \text{ ps}$$

The measured value is **in agreement with the SM prediction** and compatible with the previous LHCb results at 2.1σ and is **twice more precise**

We present two recent CMS results on the CP violation and lifetime measurements:

- First CMS measurement of CP violation in charm
- The most precise measurement of effective lifetime of the $B_S^0 \rightarrow J\psi K_S^0$

CMS recent contributions to flavor physics prove that it can be one of the leading actors in such areas as rare decays, CP violation measurements and spectroscopy

Run 3 will provide unique opportunities thanks of a revamped trigger strategy, which will lead to the collection of an unprecedented amount of data suitable for flavor physics studies

Thank you!

1. [PRD92\(2015\)054036](#)
2. [PRL122\(2019\)211803](#)
3. [PRL119\(2017\)171801](#)
4. [Nucl.Phys.B\(2013\)873](#)

Backup

CMS DETECTOR

Total weight : 14,000 tonnes
Overall diameter : 15.0 m
Overall length : 28.7 m
Magnetic field : 3.8 T

STEEL RETURN YOKE
12,500 tonnes

SILICON TRACKERS
Pixel ($100 \times 150 \mu\text{m}$) $\sim 1\text{m}^2 \sim 66\text{M}$ channels
Microstrips ($80 \times 180 \mu\text{m}$) $\sim 200\text{m}^2 \sim 9.6\text{M}$ channels

SUPERCONDUCTING SOLENOID
Niobium titanium coil carrying $\sim 18,000\text{A}$

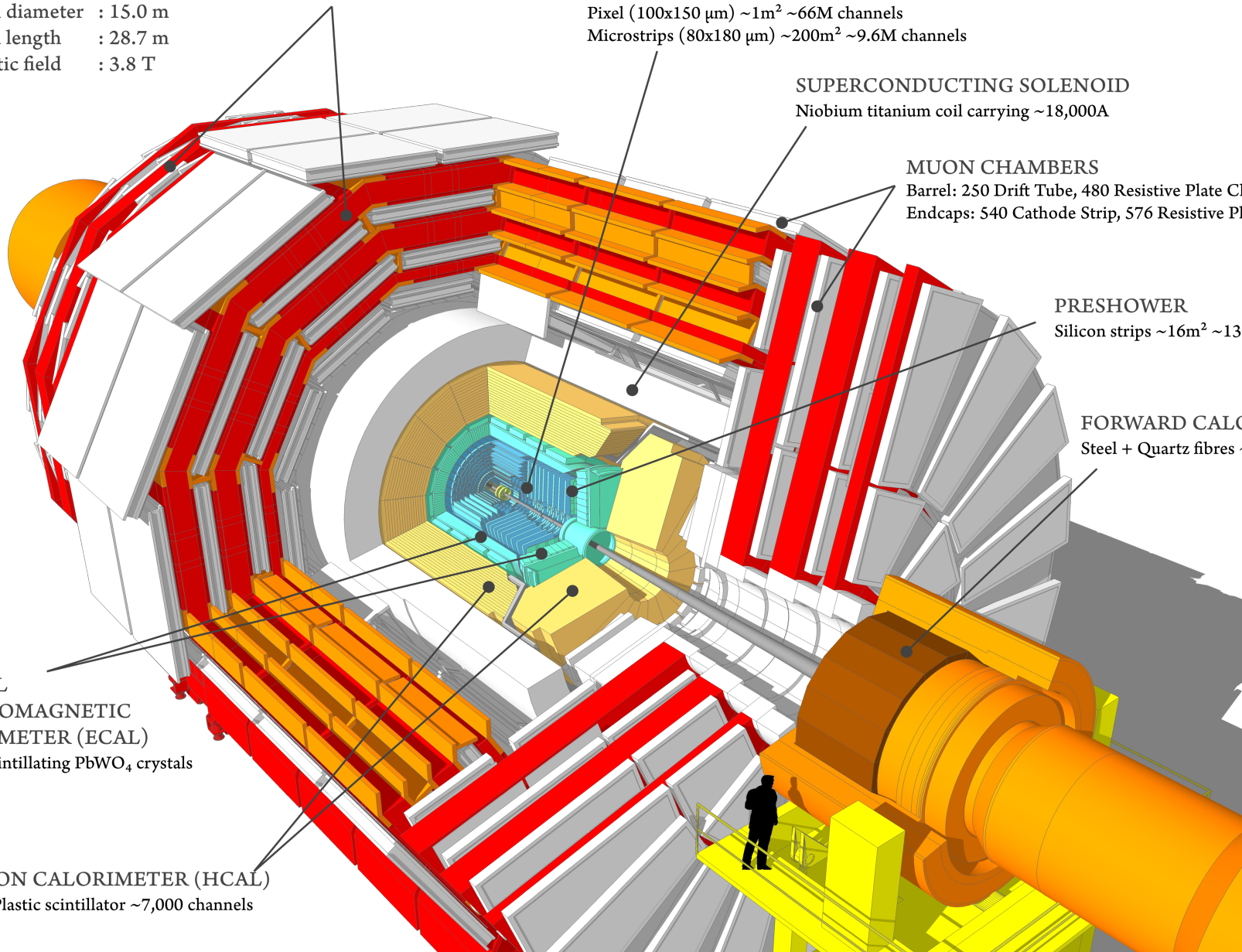
MUON CHAMBERS
Barrel: 250 Drift Tube, 480 Resistive Plate Chambers
Endcaps: 540 Cathode Strip, 576 Resistive Plate Chambers

PRESHOWER
Silicon strips $\sim 16\text{m}^2 \sim 137,000$ channels

FORWARD CALORIMETER
Steel + Quartz fibres $\sim 2,000$ Channels

CRYSTAL
ELECTROMAGNETIC
CALORIMETER (ECAL)
 $\sim 76,000$ scintillating PbWO_4 crystals

HADRON CALORIMETER (HCAL)
Brass + Plastic scintillator $\sim 7,000$ channels



A dedicated data set corresponding to the integral $L = 41 \text{ fb}^{-1}$ is used

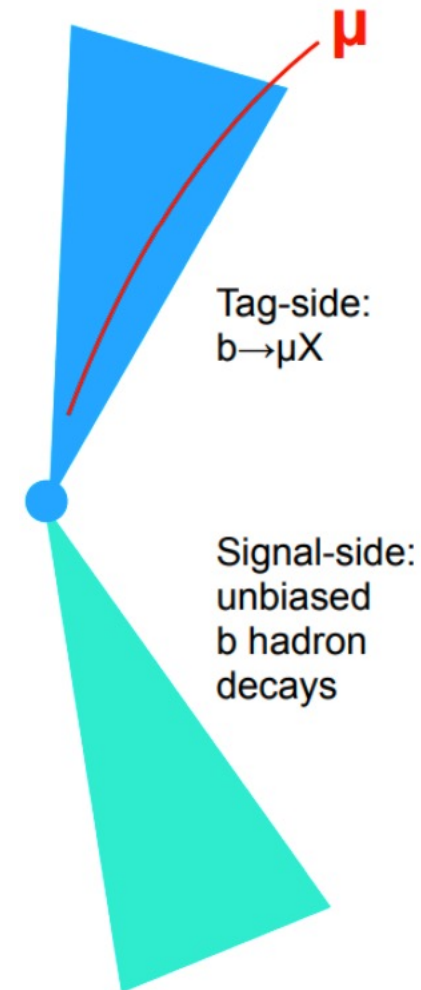
A set of single muon triggers with different thresholds on p_T^μ and impact parameter are used

Due to these thresholds, most ($\sim 75\text{-}80\%$) of the events in dataset come from beauty semi-leptonic decays $b \rightarrow \mu X$

Almost every time $b \rightarrow \mu c \nu X$

The p_T^μ cut at trigger level: 7-12 GeV D has a high p_T , as both c and μ come from energetic b-hadron

Thus, b-parking has $O(10^{10})$ events with charm hadrons with relatively high p_T it is perfect for CPV search



Variable	Requirement
p_T of tagging pion from $D^{*\pm} \rightarrow D\pi^\pm$	$> 0.35 \text{ GeV}$
η of tagging pion from $D^{*\pm} \rightarrow D\pi^\pm$	$-1.2 < \eta < 1.2$
$p_T(K_S^0)$	$> 2.2 \text{ GeV}$ and $> 1.0 \text{ GeV}$
$P_{vtx}(D\pi^\pm)$	$> 5\%$
$P_{vtx}(K_S^0 K_S^0)$	$> 1\%$
$P_{vtx}(\pi^+ \pi^-)$ for $K_S^0 \rightarrow \pi^+ \pi^-$	$> 1\%$
D^0 vertex displacement from the PV in xy	$> 2 \text{ s.d.}$
D^0 vertex displacement from the PV in xyz	$> 9 \text{ s.d.}$
K_S^0 vertex displacement from the D^0 vertex in xyz	$> 9 \text{ s.d.}$ and $> 7 \text{ s.d.}$
angle between D^0 momentum and displacement from PV in xyz	$< 0.205 \text{ rad}$
angle between D^0 momentum and displacement from PV in xy	$< 0.237 \text{ rad}$
angle between D^0 momentum and displacement from BX in xy	$< 0.237 \text{ rad}$

$$\begin{aligned}\tau(J\psi K_S^0) &\equiv \frac{\int_0^\infty t \cdot \left(\Gamma_{B_S^0 \rightarrow J\psi K_S^0} + \Gamma_{\overline{B_S^0} \rightarrow J\psi K_S^0} \right) dt}{\int_0^\infty \left(\Gamma_{B_S^0 \rightarrow J\psi K_S^0} + \Gamma_{\overline{B_S^0} \rightarrow J\psi K_S^0} \right) dt} \\ &= \frac{\tau_{B_S^0}}{1 - y_S^2} \left(\frac{1 + 2A_{\Delta\Gamma} y_S + y_S^2}{1 + A_{\Delta\Gamma} y_S} \right),\end{aligned}$$

Where $y_S = \tau_{B_S^0} \Delta\Gamma / 2$ – normalized decay width difference

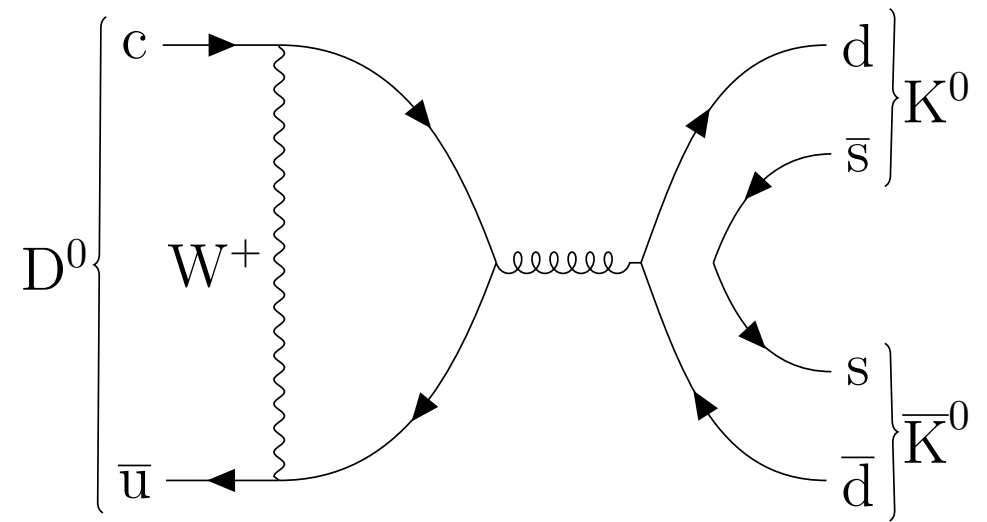
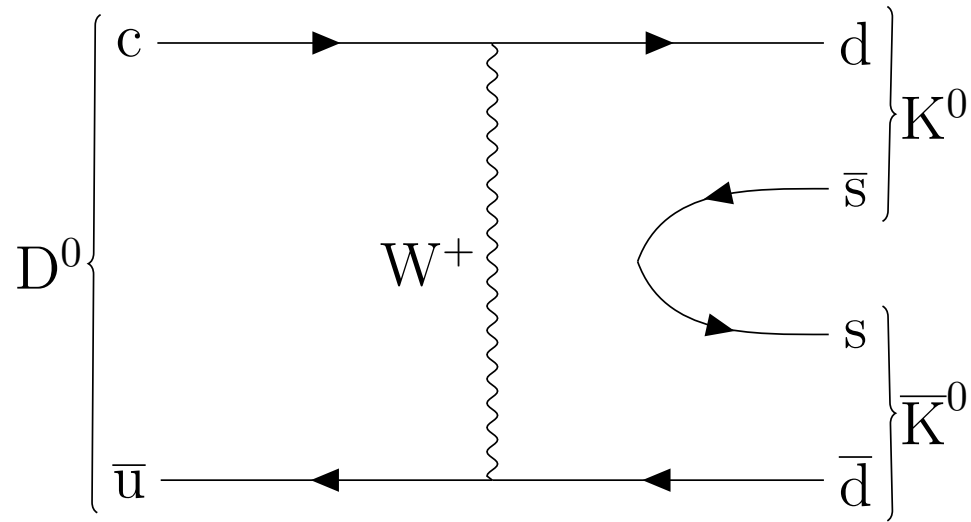
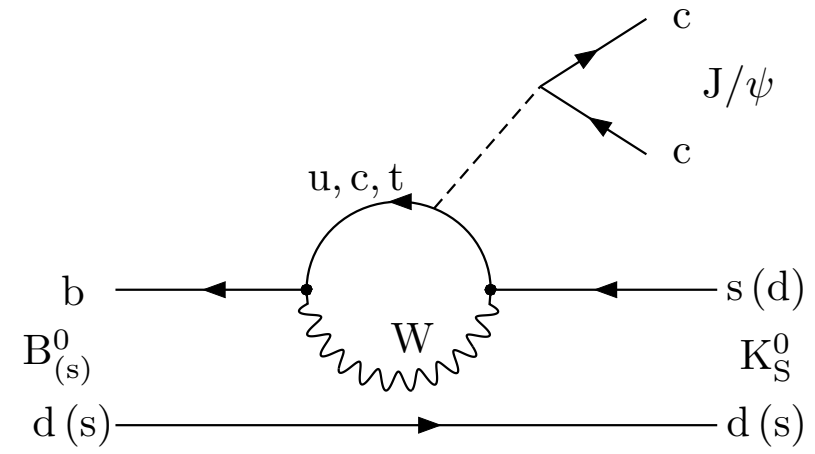
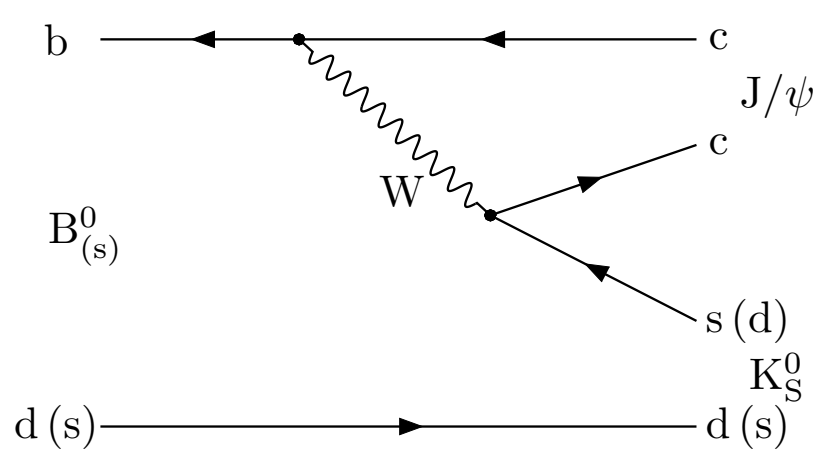
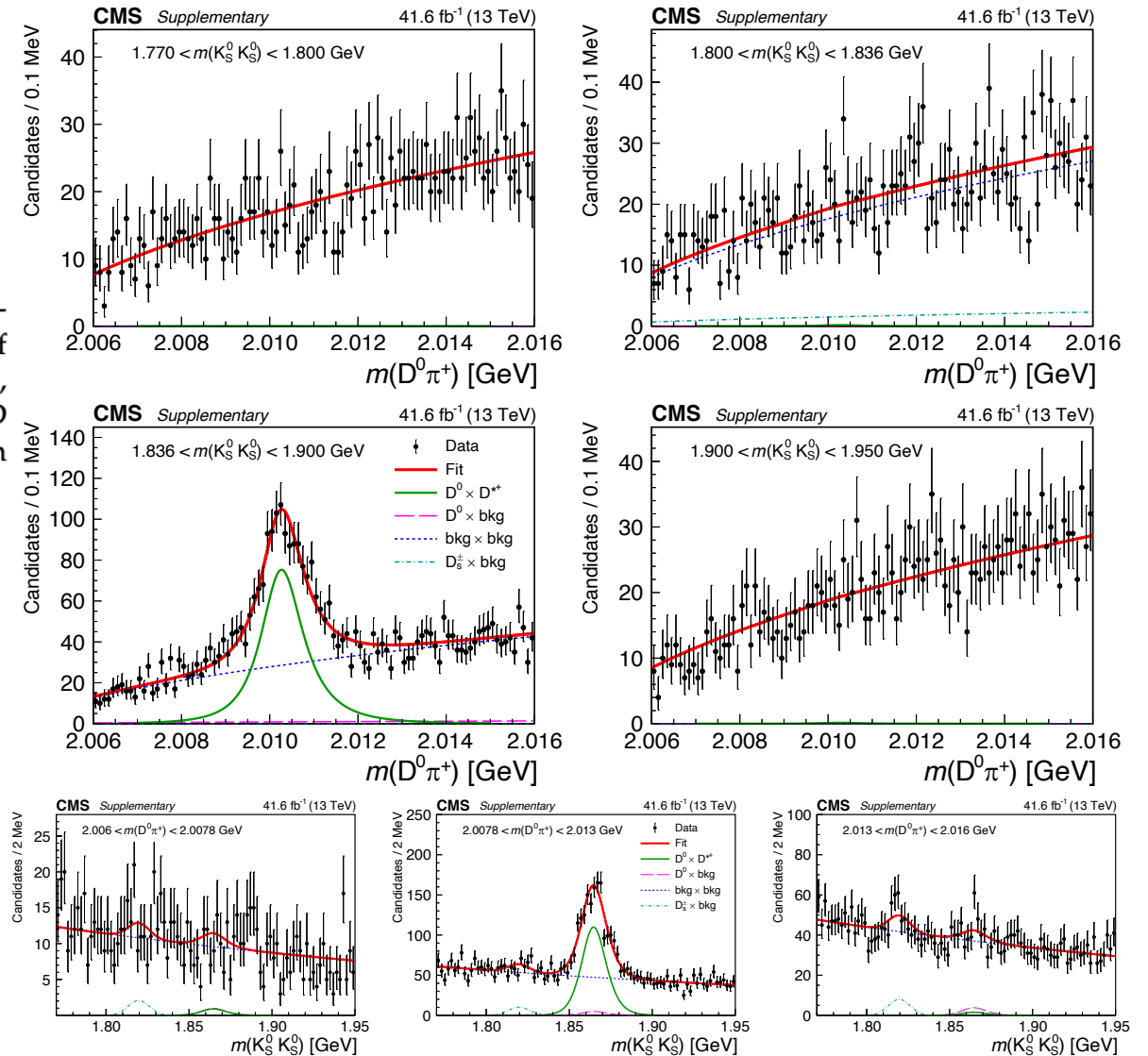


Figure A.1: Results of the 2D fit to the $m(D\pi^\pm) \times m(K_S^0 K_S^0)$ for the signal channel, D^{*+} candidates. Upper and middle rows show 1D projections of the 2D fit on $m(D^0\pi^+)$ in ranges of $m(K_S^0 K_S^0)$: left sideband (upper left), region of $D_s^\pm \rightarrow K_S^0 K_S^0 \pi^\pm$ contamination (upper right), signal region of $K_S^0 K_S^0$ (middle left), and right sideband (middle right). Lower row shows 1D projections of the 2D fit on $m(K_S^0 K_S^0)$ in ranges of $m(D^0\pi^+)$: left sideband (left), signal region of $D^0\pi^+$ (center), and right sideband (right).



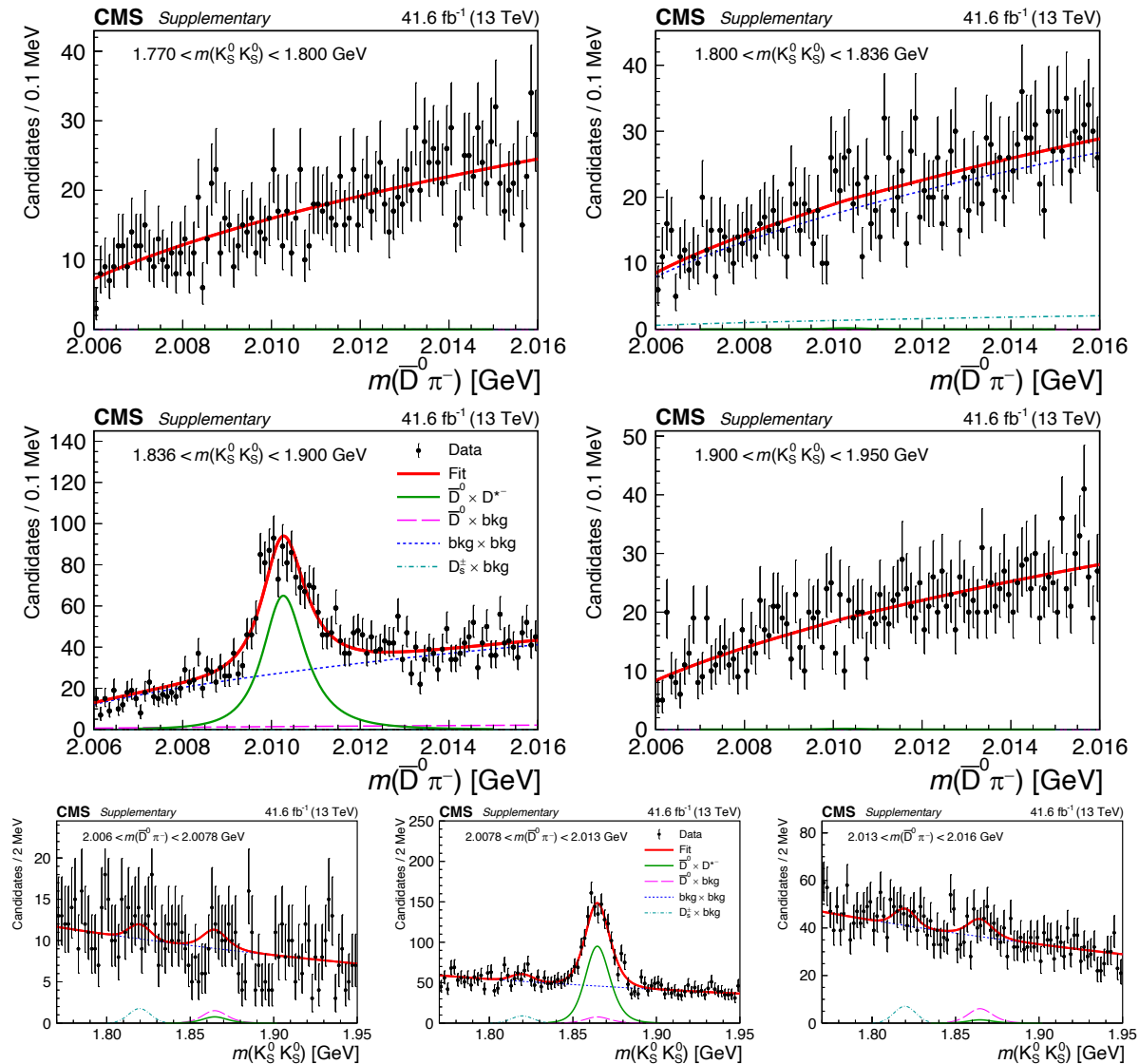
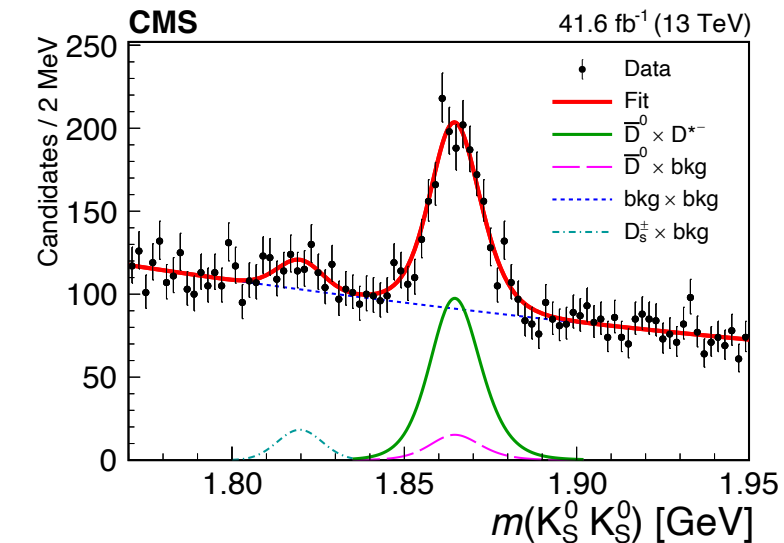
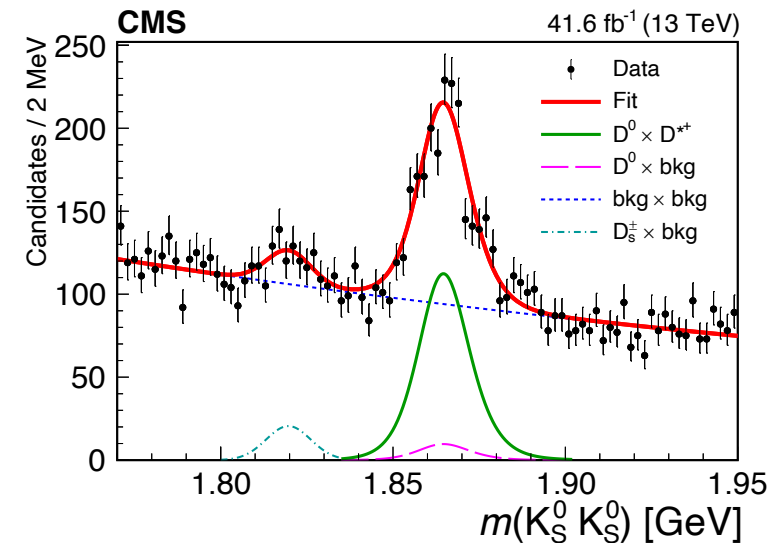
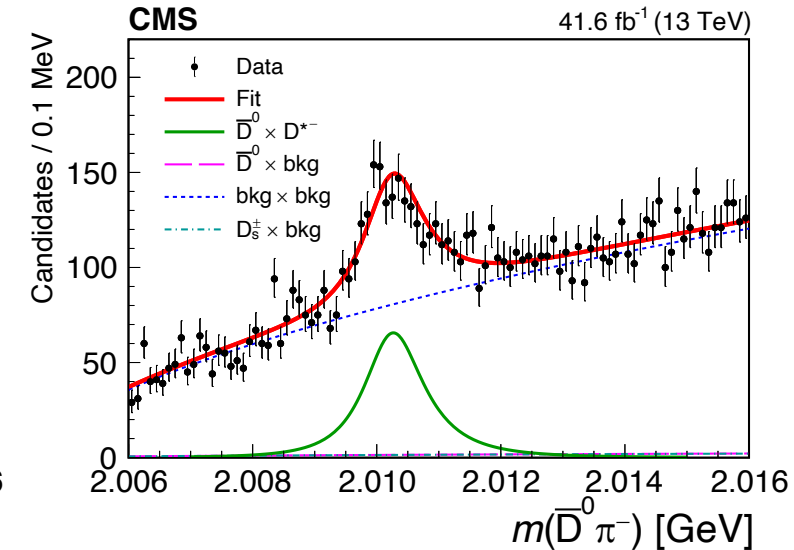
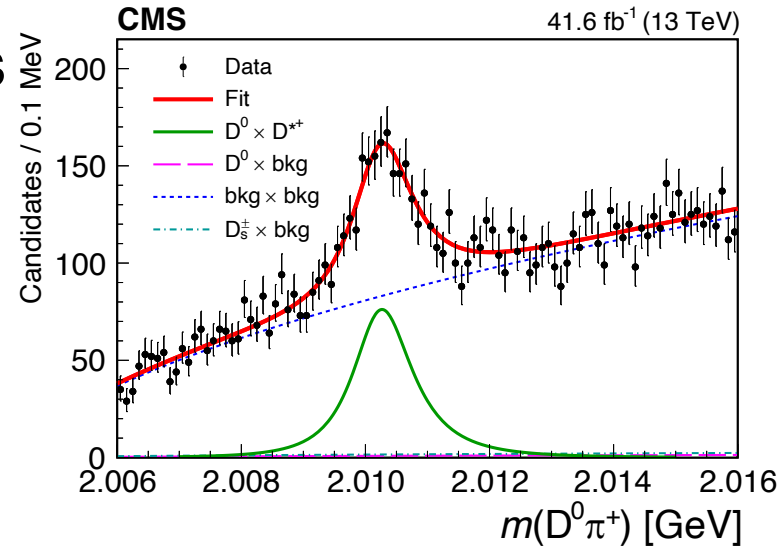


Figure A.2: Results of the 2D fit to the $m(D\pi^\pm) \times m(K_S^0 K_S^0)$ for the signal channel, D^{*-} candidates. Upper and middle rows show 1D projections of the 2D fit on $m(\bar{D}^0 \pi^-)$ in ranges of $m(K_S^0 K_S^0)$: left sideband (upper left), region of $D_s^\pm \rightarrow K_S^0 K_S^0 \pi^\pm$ contamination (upper right), signal region of $K_S^0 K_S^0$ (middle left), and right sideband (middle right). Lower row shows 1D projections of the 2D fit on $m(K_S^0 K_S^0)$ in ranges of $m(\bar{D}^0 \pi^-)$: left sideband (left), signal region of $\bar{D}^0 \pi^-$ (center), and right sideband (right).

The invariant mass distributions for D^{*+} candidates (left) and D^{*-} candidates (right), with the $m(D\pi^+)$ distributions in the upper row and the $m(K_S^0 K_S^0)$ distributions in the lower row.

Projections of the simultaneous 2D fit are also shown

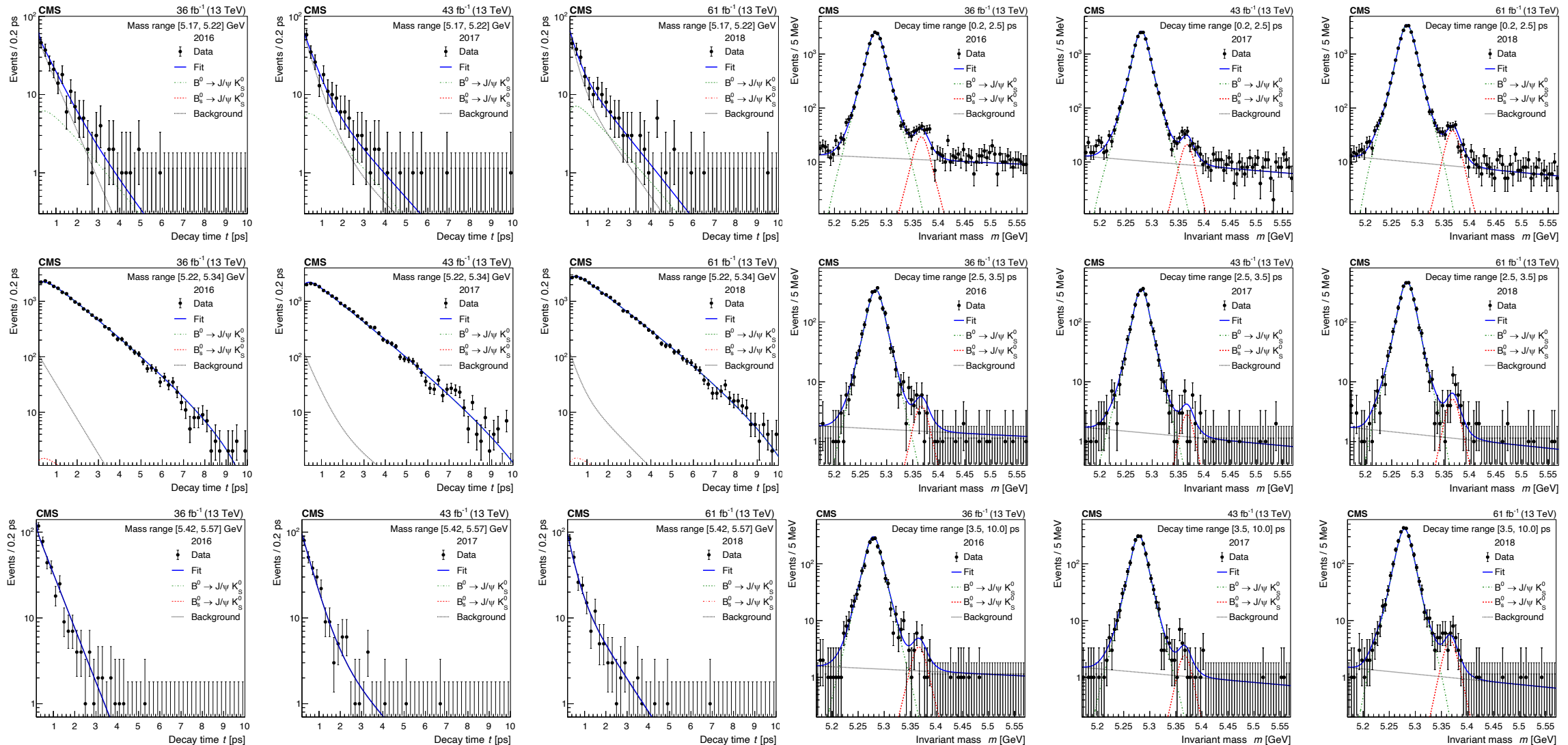


Source	Uncertainty (%)	Variable	Requirement
$m(D\pi^\pm)$ signal model	0.10	$ \eta $ of the tagging pion from $D^{*\pm} \rightarrow D\pi^\pm$	<1.2
$m(D\pi^\pm)$ background model	0.02	p_T of the tagging pion from $D^{*\pm} \rightarrow D\pi^\pm$	>0.35 GeV
$m(K_S^0 K_S^0)$ signal model	0.04	$p_T(K_S^0)$	>2.2 and >1.0 GeV
$m(K_S^0 K_S^0)$ background model	0.02	K_S^0 vertex displacement significance from the D^0 vertex in xyz	>7 and >9
$m(K_S^0 K_S^0)$ fit range	0.06	D^0 vertex displacement significance from the PV in xy	>2
Reweighting	0.09	D^0 vertex displacement significance from the PV in xyz	>9
Total	0.16	$P_{\text{vtx}}(D\pi^\pm)$	$>5\%$
		$P_{\text{vtx}}(K_S^0 K_S^0)$	$>1\%$
		$P_{\text{vtx}}(\pi^+ \pi^-)$ for $K_S^0 \rightarrow \pi^+ \pi^-$	$>1\%$
		Angle between D^0 momentum and displacement from PV in xyz	<0.205 rad
		Angle between D^0 momentum and displacement from PV in xy	<0.237 rad
		Angle between D^0 momentum and displacement from beamline in xy	<0.237 rad

Decay	N	χ^2 (x axis)	χ^2 (y axis)	Decay	N	χ^2 with 100 bins
$D^{*+} \rightarrow D^0 \pi^+$	1095 ± 46	77	90	$D^{*+} \rightarrow D^0 \pi^+$	$944\,800 \pm 3\,500$	78
$D^{*-} \rightarrow \bar{D}^0 \pi^-$	951 ± 44	93	62	$D^{*-} \rightarrow \bar{D}^0 \pi^-$	$930\,150 \pm 3\,400$	93

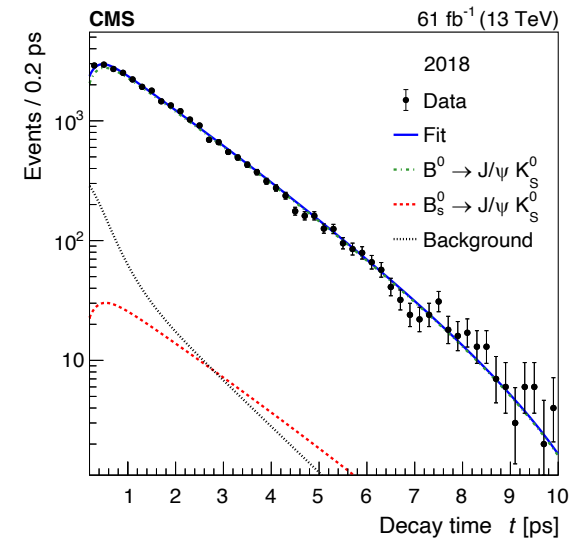
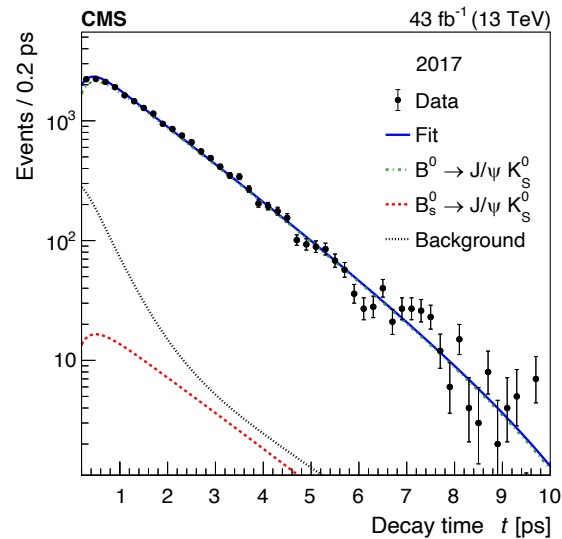
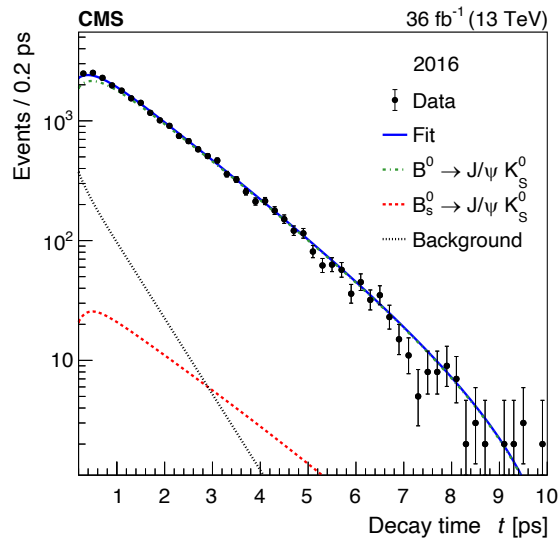
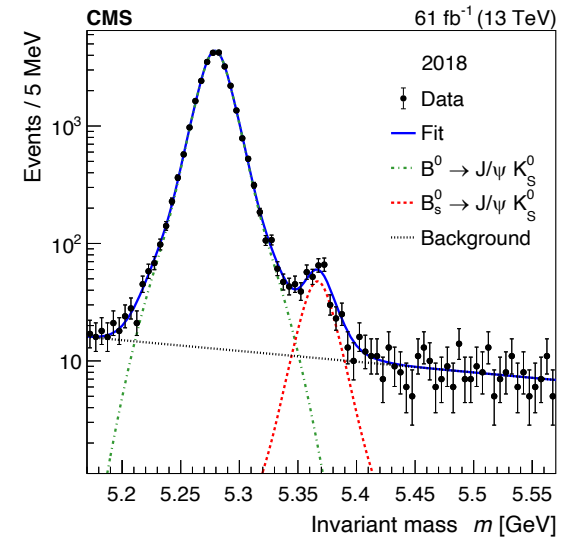
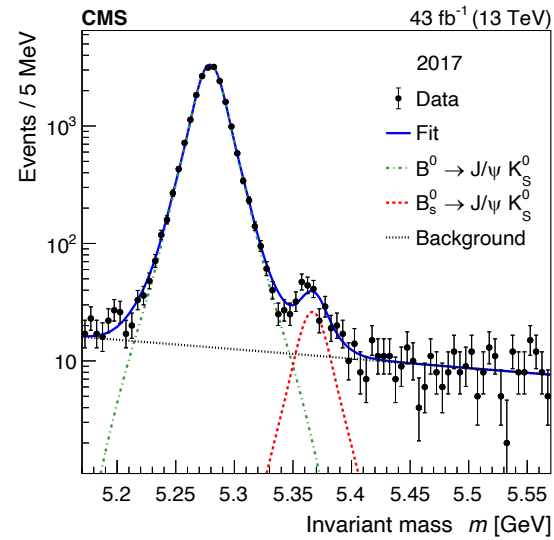
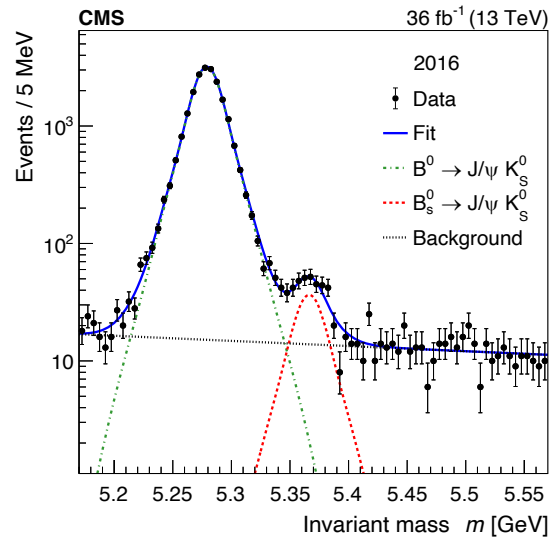
Subrange projection plots

29



Projection plots from the 2D UML fits

30



Source	Value (ps)
Limited MC event count	0.006
Efficiency modeling	0.002
Signal and background invariant mass model	0.022
Background decay time model	0.014
Invariant mass shape variation	0.004
Different fit strategy	0.006
Deviation in control channel lifetime	0.004
Total	0.028